Quantitative Analysis of Urban Polycentric Interaction Using Nighttime Light Data: A Case Study of Shanghai, China

Yue Tu, Zuoqi Chen, *Member, IEEE*, Congxiao Wang, Bailang Yu, *Senior Member, IEEE*, and Bingjie Liu

***Abstract*—The urban polycentric structure is connected to the economy and enormously impacts socioeconomic development and policies. Unlike traffic data and big geographic data, remote sensing data have shown an accessible way to measure urban spatial interaction. However, most existing studies only focused on the interaction among cities rather than within cities. Meanwhile, the urban spatial interaction, which should be directional, was always expressed as an undirected graph. Therefore, this article developed a network-based radiation model using nighttime light remote sensing data and mapped a directed interaction network (inward and outward direction) among urban centers. Taking the region within the outer ring of Shanghai as an example, the taxi trajectory data were adopted to validate the result with the R^2 of 0.61. We discovered that: the urban polycentric interaction network is dumbbell-shaped with an east-west development corridor crossing the main center and connecting two main urban center clusters. The in-strength and out-strength interaction of each urban center have a similar distribution. The urban centers with higher in-strength and out-strength are mainly concentrated toward the main center, especially in the east-west direction. At the urban center level, the total inward interaction is slightly higher than the total outward interaction of most urban centers. Spatially, an unbalanced distribution was found. In summary, our proposed method effectively indicates the urban polycentric interaction and is applicable to other regions since it requires no arbitrary parameters and the input data (e.g., nighttime light data) is readily available.**

***Index Terms*—Adjusted radiation model, nighttime light data (NTL), NPP-VIIRS, urban centers.**

I. Introduction

With the accelerating pace of urbanization, many changes happened in cities for good or for bad, such as the rural–urban migration, the population growth, and the spatiotemporal dynamics of urban expansion [1]–[3]. In the process of urbanization, the spatial distribution and interaction among cities evolve and transform [4]. The urban spatial interaction has gradually changed from single mobility to an integrated mobility containing many urban factors, such as commuting, commerce, intra-day mobility and call patterns, and so on [5], [6]. Also, the urban spatial interaction among cities can measure and reflect the intensity of the relationship between cities. A growing body of literature focuses on regional spatial interaction and attempts to measure and evaluate their structure and characteristics [7]–[9]. Many researchers have explored the spatial interaction between cities [5], [10], [11] by analyzing the spatial distribution of university students [12] and participation in higher education [13], checking improvement in energy efficiency savings [9], monitoring operational performance [14], and so on. It has been argued that urban spatial interaction plays a vital role in urbanization and has a significant impact on urban socioeconomic development [15]. Therefore, how to measure the urban spatial interaction becomes a crucial challenge for future studies.

Existing research for the measurement of urban spatial interaction can be divided into three major categories in terms of data sources. The first category relies on the traffic data from different transportations, such as airlines [16]–[18], railways [19], highways [20], and sea transportation [21]. Except for the data above, commuting data [22], migrations, [23], [24], and travel data [17], [25] are the second category, which is obtained from social media, cell phone signaling, or smart card. Unlike traditional tangible datasets, the abstract information flow also becomes the third data source for urban spatial interaction, e.g., the business contact data [26] and Sina microblog [27]. The above data can directly illustrate the directed interaction between two geographical entities at a fixed spatial scale. For example, most of the studies using these data were at the urban agglomeration or urban scale [5], [15], [28], and a few of the studies are focused on the interaction at a finer scale but for a small region [29], due to the limitation of data collection.

To fill this gap, we need to find an alternative data source that is more economical and efficient. Previous studies have proven that remote sensing technology can record the basic state information on the earth [30]; thus, it helps in sustainable urban construction and supports establishing an intelligent urban planning system [31]. Nighttime light data (NTL), taking advantage of the value of light brightness to reflect urban information directly,

Manuscript received August 29, 2021; revised November 2, 2021 and December 12, 2021; accepted December 15, 2021. Date of publication December 21, 2021; date of current version January 20, 2022. This work was supported in part by the National Natural Science Foundation of China under Grant 41871331 and Grant 41801343, in part by the China Postdoctoral Science Foundation under Grant 2020M671921, in part by the Major Program of National Social Science Foundation of China under Grant 17ZDA068, and in part by the Fundamental Research Funds for the Central Universities of China. *(Corresponding author: Zuoqi Chen.)*

Yue Tu, Zuoqi Chen, and Bingjie Liu are with the Key Laboratory of Spatial Data Mining and Information Sharing of Ministry of Education, National and Local Joint Engineering Research Center of Satellite Geospatial Information Technology, Academy of Digital China,Fuzhou University, Fuzhou 350108, China (e-mail: tycrs1996@163.com; zqchen@fzu.edu.cn; lbj012@126.com).

Congxiao Wang and Bailang Yu are with the Key Laboratory of Geographic Information Science (Ministry of Education), East China Normal University, Shanghai 200241, China, and also with China and School of Geographic Sciences, East China Normal University, Shanghai 200241, China (e-mail: cxwang1992@126.com; blyu@geo.ecnu.edu.cn).

Digital Object Identifier 10.1109/JSTARS.2021.3137167

can monitor land surface conditions at various spatial scales on continuous spatial coverage and different data storage ranges. In recent studies, NTL has shown a diverse ability to explore urban development. NTL observations record light emissions from the earth's surface at night [32]. Many researchers have documented the relationship between NTL and other issues, such as urban range identification, expansion and extraction [33]–[36], urban polycentric detection [37], regional economy and population estimation [38]–[41], environmental pollution assessment [42], [43], and natural disaster evaluation [44], [45]. Huang *et al.* [46] confirmed that NTL data could measure urban spatial interaction among cities. However, the interaction is nondirectional.

In terms of the urban spatial interaction measurement model, the most widely used is the gravity model, based on the universal gravitation formula created by Ravenstein Esq. [47]. Reilly [48] first applied the gravity model to society for measuring the spatial interaction among retail markets in cities. Researchers have developed other models based on the gravity model and achieved significant results in facilitating regional interaction analysis [49]–[55]. Several studies have provided efficient methods to measure the interaction between urban agglomerations and urban areas [5], [12], [46] instead of within urban areas, especially the polycentric areas. Singleton *et al.* [13] calibrated and tested the actual flow record of students in national schools by an integrated model comprised of the gravity model and geodemographic analysis for higher education. He *et al.* [5] explored the structure and characteristics of spatial interaction inside Wuhan urban agglomeration using a spatially explicit approach based on a comprehensive measurement system of economy, society, and environment. However, these studies continuously measured the directional spatial interaction in an isotropic way: the strength of outward interaction is the same as the strength of inward interaction due to the limitation of the gravity model. In reality, the interaction strength of a city with higher economic activities could be more robust than that of a city with lower economic activities, but not vice versa [5]. To overcome this issue, Simini *et al.* [6] developed a radiation model to derive the directed commuting and mobility fluxes among counties. This method might be preferable for obtaining the urban polycentric interaction. Existing studies have demonstrated that the NTL data is strongly associated with population and can estimate population and population surface enhancement [56], [57]. Nevertheless, the original radiation model is widely used on a large urban scale, and our objects are urban polycentric centers. It infers that the original radiation model requires a modification to deal with the urban centers.

This article aims to map the directed network of urban polycentric interaction which reflects intensity of multifactor mobility consisting of multiple urban elements based on the NTL by developing the radiation model. Specific objectives are modifying the radiation model to be suitable for the urban centers, and measuring and analyzing the urban polycentric interaction within the outer ring of Shanghai.

The rest of this article is organized as follows. Section II describes the related data and research area. In Section III, we provide an overview of the research process, including the calibration of the NTL, the identification of the urban centers and subcenters, the construction of urban polycentric interaction network, and the quantitative analysis of urban polycentric interaction network. Section IV demonstrates the visualization results, and Section V discusses the quantitative analysis results of urban polycentric interaction relationship in the context of urban areas. Finally, Section VI concludes the article.

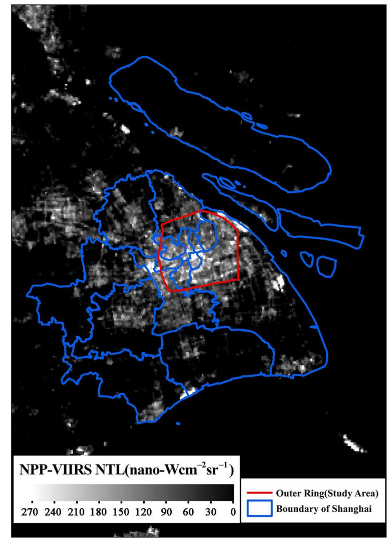

Fig. 1. Geographical location and the NPP-VIIRS of April 2015.

II. Study Area and Data

A. Study Area

Shanghai is located in the estuary of the Yangtze River in Eastern China. As one of the four municipalities, Shanghai is the core city of the National Central City, megacity, Shanghai Metropolitan Area. It is also China's international economic, financial, trade, shipping, scientific, and technological innovation center approved by the State Council. Since the Chinese government adopted the reform and opening policies at the end of the 1970s, Shanghai has experienced fast population growth and rapid urbanization in recent decades. Since 1991, Shanghai has experienced rapid urban transformation and development. Correspondingly, the improvement of polycentricity and periphery has become a momentous tactic in the urban master plan of Shanghai City [58], and the urban areas have undergone an enormous spatial expansion. Shanghai's polycentric areas have emerged as time goes on, and the new urban form with increasing significance has attracted the attention of many researchers [58].

Therefore, taking Shanghai as the example to evaluate our proposed urban polycentric interaction measurement and analyze the characteristics of urban polycentric interaction is typical and valuable.

B. Data

The version 1 monthly NPP-VIIRS DNB cloud-free composite data of April 2015 was used in this article (See Fig. 1). The NPP-VIIRS NTL composite data were reprojected to the Mercator Positive Axis Isometric cylindrical projection with

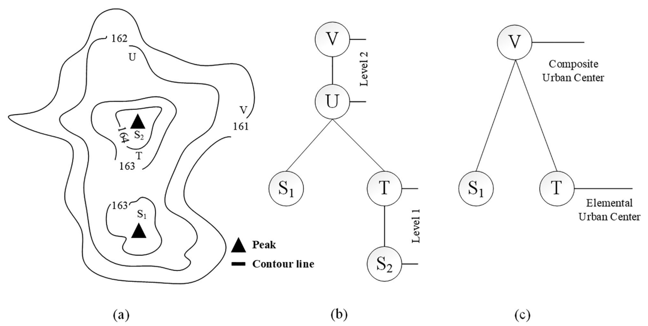

Fig. 2. Illustration of the urban center detection using the contour tree method. (a) Contour map of NTL intensity. (b) Regular contour tree. (c) Simplified contour tree.

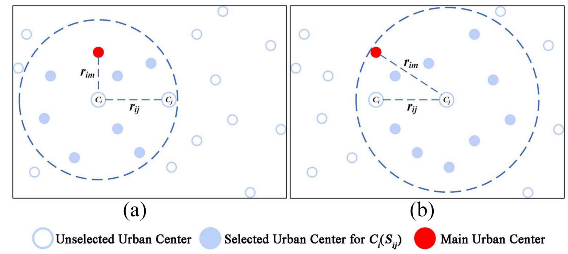

Fig. 3. Two scenarios of S_{ij} for the interaction (T_{ij}) from the ith center (C_i) to the jth center (C_j).

a pixel size of 500 m. To eliminate abnormal light detection associated with fire, volcano, and background noise, we adopted the NPP-VIIRS mutual correction method proposed by Shi *et al.* [59]. All the negative pixels were assigned as 0.

Taxi OD flow data from April 1 to April 3, 2015, were used in this article as reference data to evaluate our measurement of urban polycentric interaction since some scholars have mentioned that taxi data sets can reveal the interaction within cities [60]. The dataset records the beginning and ending points of each taxi trip, which is easy to count the number of trips between two urban centers. Due to the limitation of taxi OD data access, the data we got only covered the regions within the outer ring of Shanghai. So, the further evaluation and analysis were only within this region.

III. Methodology

A. Urban Polycentric Identification

The localized contour tree method proposed by Chen *et al.* [37] was adopted to identify urban polycentric structures based on the corrected NTL data. This method proposed a topographical metaphor of a mount to identify the urban polycentric centers.

The generation of the localized contour tree method comprises of four parts: generating the NTL contour map; searching for seed contour; generating regular contour trees; and simplifying contour trees.Fig. 2 illustrates how to build up a regular contour tree and a simplified contour tree based on a sample NTL intensity contour map. This sample region has two elemental urban centers (*S1* and *T*), included in a larger composite urban center (*V*). The NTL data was firstly converted to contour lines with a contour interval of 1 nano-Wcm^{-2}sr^{-1} [see Fig. 2, (a)]. Then, the "seed" contour line is defined as one isoline that does not contain other contour lines and contains a local highest point. In Fig. 2, contours *S1* and *S2* are the only two seed contour lines. Each "seed" contour line may be the starting node of a local contour line tree of a single plant. In a polycentric city, there are usually multiple "seed" contours, which are regarded as first-order nodes. These "seed" contours are treated as level 1 nodes and the starting point of the local contour tree algorithm and searching outwards one by one based on the contour tree. If the contour outwards closest contour contains only the "seed" contour and its value is lower than the "seed" contour value, it is considered to have the same rank as the "seed" contour. If the closest contour outwards of a "seed" contour contains contours other than that of the "seed" contour, the contour will be assigned a higher rank than the "seed" contour. For instance, nodes T and *S*2, in Fig. 2, both remain with the level-1 nodes. Contour *U* contains contours *S1* and *T*, the two independent nodes in the regular contour tree. Thus, contour *U* is identified as level 2. A conventional contour map will be obtained by iterating the process until all contours are retrieved and discriminated. All the regions circled by each contour with the lowest rank were treated as the urban centers [see Fig. 2(b)]. For the details, please refer to Chen *et al.* [37].

B. Construction of Urban Polycentric Interaction Network

Since the radiation model has been employed widely in measuring the field of fluxes, we focused on its modification and application in measuring the urban polycentric interaction. For the details of its principle and mechanism, please refer to Simini *et al.* [6]. Generally, the radiation model can be expressed as

$$T_{ij} = m_i \frac{m_i n_j}{(m_i + S_{ij})(m_i + n_j + S_{ij})}$$
$$(i, j = 1, 2, \ldots, n, i \neq j) \tag{1}$$

where m_i and n_j represent a social-economic index (e.g., the total population in Simini *et al.* [6], and total NTL intensity in this article) of *i*th and *j*th geographical entities (e.g., counties in Simini *et al.* [6], and urban centers in this article). T_{ij} denotes the fluxes between *i*th entity and *j*th entity. In this article, it refers to the interaction from the *i*th center to the *j*th center. Traditionally, the S_{ij} denotes the total value of the social-economic index for all urban centers whose distance from the *i*th center is less than the distance between the *i*th center and the *j*th center (r_{ij}). In this article, we believe that the main center plays a key role in a polycentric structure. The interaction between any two subcenters must also be impacted by the main center, no matter how far they are from the main center. Therefore, to calculate the S_{ij}, we set two scenarios according to the comparison between the r_{ij} (distance between the *i*th and the *j*th center) and the r_{im} (distance between the *i*th center and the main center). In Fig. 3(a), once the r_{ij} is larger than the r_{im}, the S_{ij} is the total NTL intensity of urban centers (blue circles in Fig. 3) whose distance from the *i*th center is less than r_{ij} but excluded m_i and n_j. Otherwise, the S_{ij} is the total NTL intensity of urban centers whose distance from the ith center is less than r_{im}, and excluded m_i and n_j, as shown in Fig. 3(b).

Since the S_{ij} in this article is not the same as the S_{ji} in Simini *et al.* [6], the modified radiation model could measure the directed interaction between two urban centers, a matrix T (n by n) can be obtained. Given the ith urban center, T_{ij} means the outward interaction to the jth urban center, while T_{ji} indicates the outward interaction from the jth urban center.

C. Quantitative Analysis of Urban Polycentric Interaction Network

1) Model Validation: To verify the accuracy of urban polycentric interaction in this article, we fitted the interaction and taxi OD data. We counted the total number of taxi trips between any two centers to generate a matrix D with the same size as the matrix T. The value R^2 denotes the accuracy of the calculated result. The formula for calculating the linear regression model is

$$D = wT + c \tag{2}$$

where w is the regression coefficient, and c shows the intercept obtained by the regression analysis based on the sample pixels.

2) Node Characteristic Analysis: Three indices are used to evaluate the characteristic of each urban center, in-strength, out-strength, and the ratio of in-strength to out-strength. In (3) and (4), the in-strength calculates the total inward interaction to the ith urban center, while the out-strength calculates the total outward interaction from the ith urban center. In (5), R_i represents the ratio of in-strength to out-strength for the ith urban center, and $R_i > 1$ means the ith urban center is an area where there is a growth pole, still attracting human beings or economic activities, while $R_i < 1$ means the urban center is an area is shrinking.

$$T_i^{\text{in}} = \sum_j^n T_{ji}(i, j = 1, 2, \cdots, n, i \neq j) \tag{3}$$

$$T_i^{\text{out}} = \sum_j^n T_{ij}(i, j = 1, 2, \cdots, n, i \neq j) \tag{4}$$

$$R_i = \frac{T_i^{\text{in}}}{T_i^{\text{out}}} \, (i = 1, 2, 3, \cdots, n) \, . \tag{5}$$

IV. Results

A. Urban Polycentric Centers Within the City

We extracted 13 urban centers within the outer ring of Shanghai by NTL data and the localized contour tree method. Almost all of the previously identified urban centers (red cross in Fig. 4) were detected in this article. Compared with the a previous study [37], this result is reasonable.

Based on experience, we divided the urban centers into four groups, the main center, high-tech related center, comprehensive service center, and transportation center (see Fig. 4). In particular, the urban center (No. 8) is the main center and the traditional central business district in Shanghai, located in the *Lujiazui* region. The high-tech related centers (Nos. 6, 9, and 12) were all in the *Pudong new district*. The two transportation centers were close to the Huangpu river. The remaining seven urban centers were the comprehensive centers and mainly at the west side of the main center.

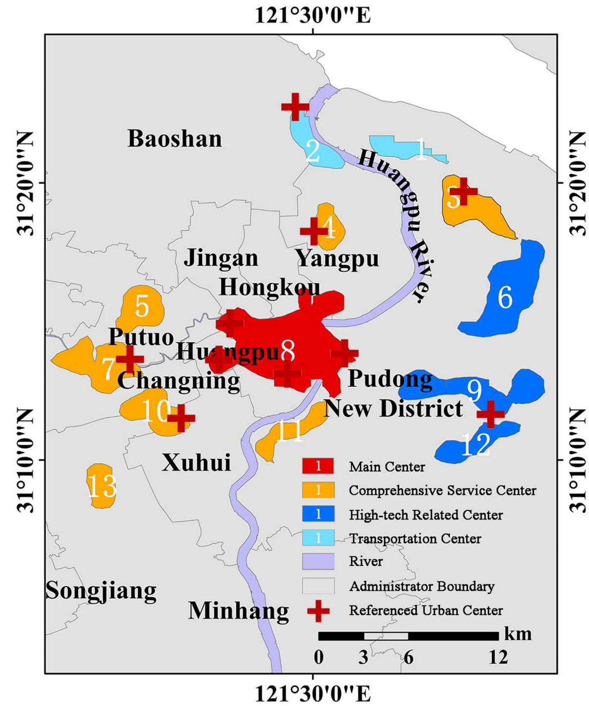

Fig. 4. Identified urban centers within the outer ring of Shanghai.

B. Urban Polycentric Interaction Network

The urban polycentric interaction network within the outer ring of Shanghai was drawn as a network graph in Fig. 5. Each urban center was a node of the network, and the interaction matrix T was an edge. The color impression from green to red stands for the variation in the intensity of urban polycentric interaction from the lowest to the highest. Each subfigure presents the outward interaction from all urban centers to a specific urban center. For instance, Fig. 5(a) illustrates the outward interaction from all urban centers to the No. 1 urban center.

Generally, we observed that the mapped urban polycentric interaction network can be described as a dumbbell-shaped development pattern (see Fig. 6, yellow line). The main center (No. 8) was a super core that had the strongest interaction with the other urban centers, particularly with the urban centers to its east (Nos. 3, 6, and 9) and west side (Nos. 5, 7, and 10), as shown in Fig. 5(h). Consequently, an east-west development corridor was formed and heavily connected two main clusters. One cluster consists of Nos. 5, 7, and 10 urban centers [see Fig. 5(g)], and the second cluster was formed from Nos. 3, 6, 9, and 12 urban centers [see Fig. 5(f) and (i)].

However, the urban centers were relatively isolated in the north or south of the study area and did not form a significant cluster. For instance, the Nos. 1, 2, and 13 urban centers had weak inward and outward interaction with the rest of the urban centers, even with the main center [see Fig. 5(a), (b), and (m)].

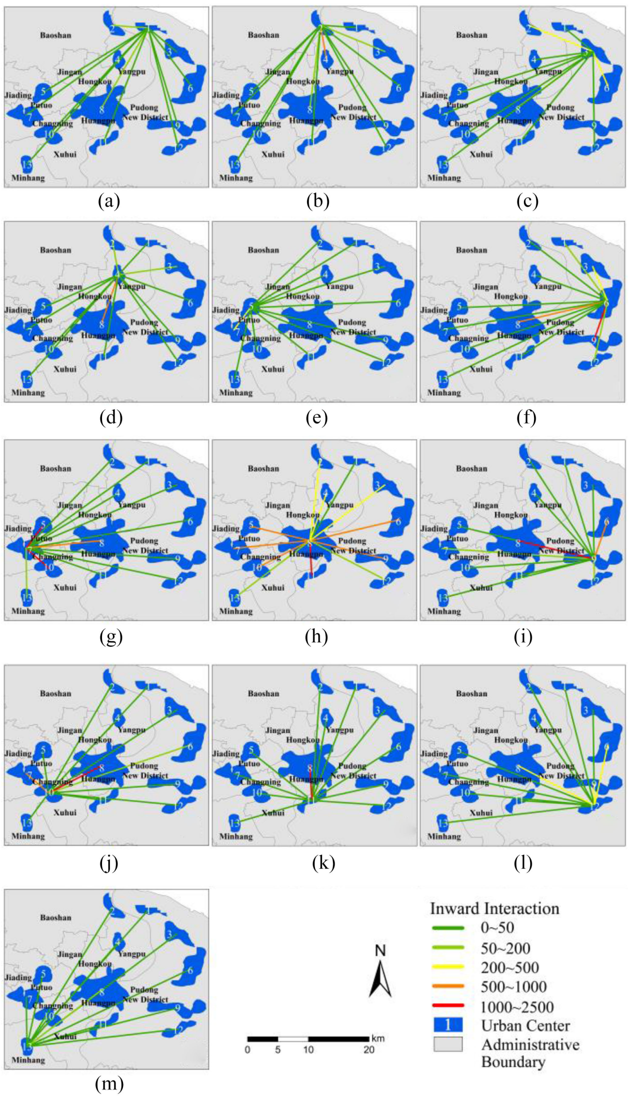

Fig. 5. Inward interaction for each urban center.

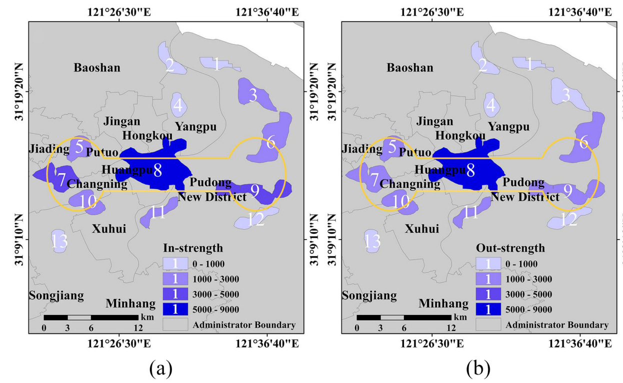

Fig. 6. In-strength (a) and out-strength (b) of each urban center (yellow line indicates the dumbbell-shaped pattern).

TABLE I
NODE ATTRIBUTE CHARACTERISTICS

Urban Center ID	In-strength	Out-strength	Ratio
1	290.16	171.02	1.70
2	948.47	738.46	1.28
3	1065.44	938.06	1.14
4	912.77	907.37	1.01
5	1186.06	1787.91	0.66
6	2746.00	2437.20	1.13
7	3559.02	2089.77	1.70
8	6217.69	8538.43	0.73
9	3071.32	2412.88	1.27
10	1883.76	2361.95	0.80
11	1611.83	1499.12	1.08
12	894.49	500.63	1.79
13	228.26	232.49	0.98

On the contrary, some urban clusters (e.g., Nos. 4 and 11) had a strong interaction with the main center, even though they had a weak interaction with most of the other urban centers [see Fig. 5(d) and (k)].

C. Characteristics of Urban Polycentric Interaction Network

The in-strength and out-strength interaction of each urban center exhibited a similar distribution when the direction of interaction from Fig. 6 and Table I are compared. The top five in-strength interaction are, in order, Nos. 8, 7, 9, 6, and 10 urban centers, with the values of 6217.69, 3559.02, 3071.32, 2746.00, and 1883.76 in sequence. For the out-strength interaction, the top five urban centers are Nos. 8, 6, 9, 10, and 7 with the values of 8538.44, 2437.20, 2412.88, 2361.95, and 2089.77, respectively.

Remarkably, the main center has the strongest in-strength and out-strength simultaneously, which means the main center has frequent population movement and economic interaction. Besides, the No. 5 urban center has the smallest ratio, with its out-strength much stronger than its in-strength, which means this urban center has a strong radiation effect and might be shrinking. By contrast, the Nos. 7 and 9 urban centers have a greater in-strength than their out-strength, which indicates that these two urban centers have a strong siphon agglomeration effect and are still attracting human beings.

Spatially, Fig. 6 shows that the urban centers with higher in-strength and out-strength are also mainly concentrated to the main center, especially in the east-west direction. However, in the north of our study area, the urban centers all have a lower interaction (both inward and outward), such as Nos. 1, 2, 3, and 4 urban centers.

Fig. 6 illustrates the source and direction of interaction mobility, reflecting the diversity of interaction mobility. Furthermore, Table I gives that the inward and outward interactions are dispersive. The ratio of in-strength to out-strength ranges from 0.66 to 1.79, and most urban centers have a ratio close to 1. Three urban centers with a ratio higher than 1.5 are Nos. 1, 7, and 12, while the four urban centers with a ratio less than 1 are Nos. 5, 8, 10, and 13.

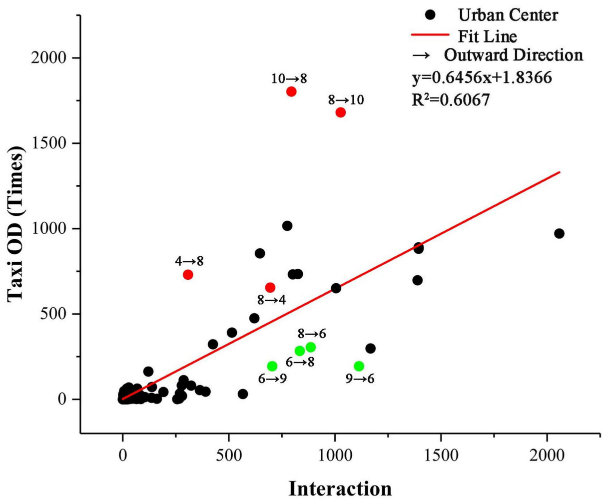

Fig. 7. Fitting results of urban polycentric interaction and taxi OD data.

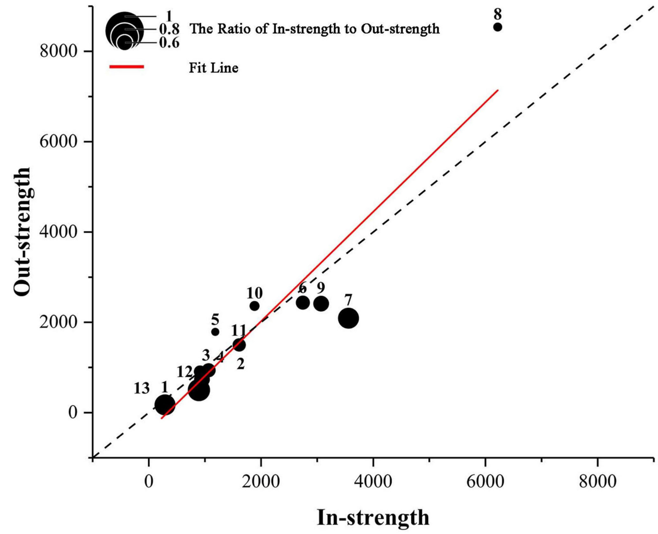

Fig. 8. Fitting results of in-strength and out-strength for each urban center.

V. Discussion

A. Accuracy Evaluation

The fitting results of the urban polycentric interaction and taxi OD data were obtained through a linear regression model. The R^2 value is 0.61 (see Fig. 7), which shows that the urban polycentric interaction fits well with the OD flow data. However, it still has some outliers, such as the red and green points in Fig. 7, which could be caused by the bias when using the taxi OD data as the reference data.

The interaction can be performed in many ways. The interaction network from the taxi OD data only records human mobility via taxi. In contrast, the interaction network from NTL data can indicate human mobility and economic interaction because the NTL data is a comprehensive indicator [61]. Therefore, the conceptual gap is the first reason why our estimation has some outliers.

Meanwhile, the taxi OD data only records the taxi trip and misses the interaction using other traffic tools (e.g., public bus, subway). The traffic tool selection is sensitive to the trip conditions, such as trip distance, weather, clients, and is a function of urban destination [62]. For example, when the trip distance is too long (e.g., Nos. 6 and 8) or too short (e.g., Nos. 6 and 9), the public bus and subway could be the primary option, rather than the taxi, which induces an overestimation in our results (the green points in Fig. 7).

Additionally, Xia *et al.* [60] has demonstrated that people tend to attend entertainment activities by taxi after working on Fridays, which means urban centers with a recreational function will experience a surge of taxi trip on Fridays. Thus, this may lead to an underestimation of interaction (the red points in Fig. 7). For instance, the No. 8 urban center is considered a center with many activities and facilities (see Fig. 4). Meanwhile, the Nos. 4 and 10 urban centers are recognized as the residential areas and population centers (see Fig. 4) and close to the No. 8 urban center. The interaction between Nos. 4 and 8 exhibits significant underestimation as well as the interaction between Nos. 10 and 8.

It must be noted that the limitation of our proposed model could also influence the accuracy. In Section V-D, we will discuss these limitations in detail.

B. Balance of Urban Polycentric Inward and Outward Interaction

In this part, we will observe the balance of the inward and outward interaction for urban centers since we have mapped the directed network of urban polycentric interaction.

At the urban center level, the total inward is slightly higher than the outward interaction (see Fig. 8). From Table I, most of the urban centers have a ratio of in-strength to out-strength (ratio for short) close to 1 and the average ratio is 1.17, which is larger than 1. Meanwhile, Fig. 8 shows a linear relationship between in-strength and out-strength at the urban center level with R^2 of 0.87 and slope of 1.21, proving that the in-strength and out-strength interaction are close to each other.

Spatially, an unbalanced distribution was found among all urban centers (see Fig. 9). The urban centers, whose ratio is larger than 1, were mainly located in our study area's middle and eastern regions, except for the No.7 urban center. The urban centers, whose ratio is smaller than 1, were mainly located in the western part, most of which are the traditional old urban centers.

C. Drivers of Urban Polycentric Interaction

By analyzing the spatial distribution and balance of interaction among urban centers, we summarized three dominant drivers.

First, the urban sphere of influence is the primary driving factor. Xia *et al.* [32] considered that the core urban area has the strongest radiation ability compared to other urban areas. In other words, the larger the urban center, the wider the urban sphere of influence. For example, the No. 8 urban center has large outward interaction from almost all urban centers [see Fig. 5(h)] since it is the main center and has the largest sphere of influence. However, the small urban centers (e.g., Nos. 2 and 5) can attract

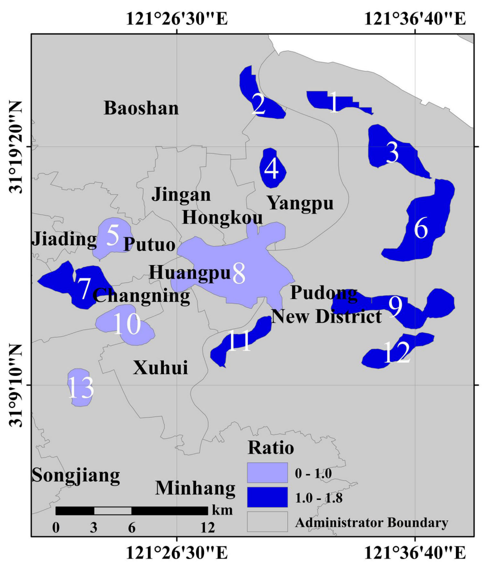

Fig. 9. Distribution for the ratio of in-strength to out-strength.

more interaction from closer urban centers (e.g., No. 4 for No. 2, and No. 7 for No. 5) than from the urban centers far away, as shown in Fig. 5(b) and (e).

Second, the distance between urban centers also impacts the interaction under specific conditions. For instance, from Fig. 5(g) and (h), No. 5 urban center has more interaction with No. 7, than No. 8, even though No. 8 has the largest attraction among all urban centers. In fact, Nos. 7 and 8 can provide almost the same services for No. 5 (see Fig. 4). Under this condition, because the distance between Nos. 5 and 7 is much shorter than that between Nos. 5 and 8, No. 5 could have a stronger connection with No. 7. Combining Chen *et al.* [37] and Giuliano and Small [63] research, the functions of the urban centers impact the surrounding urban centers and areas. It means that given an urban center, the nearest one among the urban centers with the same function would be the primary interaction object, no matter how large the urban center is.

Urbanization planning is the third driving factor. Due to the issues caused by the population and economic activity concentration, Shanghai has pursued a polycentric urban structure to decentralize human beings [37]. Meanwhile, human beings tend to choose to work where the salary is high and live where the cost is low [38], [64]. So, human beings would migrate to the subcenters. This is why the old urban centers (e.g., Nos. 8, 5, and 10) have a ratio less than 1, and some new urban centers have a ratio larger than 1. Additionally, the "1 + 3 + 9" construction of national-level industrial parks in general urban planning of Shanghai Municipality also increases urban polycentric interaction in *Pudong New District* and drives the formation of the urban center cluster.

D. Limitations and Future Perspectives

In this article, we successfully developed an effective way to measure the urban polycentric interaction based on the NPP-VIIRS NTL composite data. Nevertheless, we only focused on the interaction among urban centers. However, in reality, the region outside the urban centers, even outside our study area, could also have inward or outward interaction with the urban centers in reality. Considering the information from such a region, we will keep modifying the radiation model in future work.

Additionally, we only used the NTL data to simulate the interaction network by assuming that the nighttime light from different places has the same weight. Actually, factory and residential areas with the same nighttime light intensity should have different interactions. Therefore, the points of interest data or other geographic big data can be added as auxiliary data to help divide the urban function more carefully.

Sometimes people choose to travel by bus or private car, so it is difficult to obtain the bus frequency data and a large number of private trips were not recorded. Especially in the context of the increasing number of private cars and the increasing popularity of self-driving, the taxi OD data has substantial limitations, which lead to the deviation of its verification results (e.g., Nos. 3 to 1 and Nos. 9 to 12). Therefore, big geographic data (e.g., mobile signaling data) can be adopted as reference data in the future.

Compared with the statistical data used by traditional studies [5], the NTL data in our research is readily available and can be downloaded on the Internet for free. The modified radiation model is easy to operate and applicable to other regions since it requires no arbitrary parameters. The approach used in existing studies needs several parameters, and the process is more complex than the method we used. Our method can be applied at a flex spatial scale and offer researchers a novel way to explore the spatial connection and socioeconomic development. In the context of regional development and accelerated flow of regional elements, more regional studies need to harness the results of spatial interaction analysis at the grid-scale, such as urban land-use change simulation, urban expansion simulation, urban functional zoning, and others. The spatial interaction analysis within cities provided by our method can give regional information and references for policymakers and guide regional sustainable development. In future studies, we will further extend this method to other cities and explore the interaction between urban centers to achieve its universality.

VI. Conclusion

Polycentric communication within urban areas is becoming more common and studying the urban polycentric interaction within cities can help the future development of cities. In this article, the NTL intensity measured by satellite sensors was considered economic activity, reflecting the variation of human activity intensity. An area with strong NTL intensity indicates that it has a high level of economic development. By using the NTL data, the modified radiation model was developed to explore the urban polycentric interaction. In the case of Shanghai City, we have successfully calculated the urban polycentric interaction within the outer ring, determined the spatial distribution among them, and analyzed the characteristics of urban polycentric interaction in a directed network.

We extracted 13 urban centers within the outer ring of Shanghai by NTL data and localized contour tree method. Generally, a dumbbell-shaped development pattern was found in the urban polycentric interaction network. Besides, the total inward interaction is slightly higher than the outward interaction at the urban center level. However, spatially, the interaction among urban centers has an unbalanced distribution. The urban polycentric interaction correlates well with the taxi OD data, and the averaged R^2 is 0.61. There are outliers in the fitting results caused by the conceptual gap between the NTL and taxi OD data. We also summarized the driving factors of forming the interaction network according to the reality of urban development, such as the urban sphere of influence, the distance between urban centers, and urban development planning.

This article presents an efficient method for measuring and analyzing the urban polycentric interaction within the outer ring of Shanghai. We are convinced that this method would be widely available in some fields, such as urban planning and development assessment.

REFERENCES

[1] K. H. Zhang and S. Song, "Rural–urban migration and urbanization in China: Evidence from time-series and cross-section analyses," *China Econ. Rev.*, vol. 14, no. 4, pp. 386–400, Jan. 2003.

[2] C. He, Z. Liu, J. Tian, and Q. Ma, "Urban expansion dynamics and natural habitat loss in China: A multiscale landscape perspective," *Global Change Biol.*, vol. 20, no. 9, pp. 2886–2902, 2014.

[3] R. Lee, "The outlook for population growth," *Science*, vol. 333, no. 6042, pp. 569–573, 2011.

[4] C. Gu and J. Shen, "Transformation of urban socio-spatial structure in socialist market economies: The case of Beijing," *Habitat Int.*, vol. 27, no. 1, pp. 107–122, 2003.

[5] J. He, C. Li, Y. Yu, Y. Liu, and J. Huang, "Measuring urban spatial interaction in Wuhan Urban Agglomeration, central China: A spatially explicit approach," *Sustain. Cities Soc.*, vol. 32, pp. 569–583, 2017.

[6] F. Simini, M. C. Gonzalez, A. Maritan, and A. L. Barabasi, "A universal model for mobility and migration patterns (in English)," *Nature*, vol. 484, no. 7392, pp. 96–100, Apr. 2012.

[7] A. Maria, L. F. d. G. Henri, and J. G. M. F. Raymond, "Spatial patterns of technology diffusion: An empirical analysis using TFP," Tinbergen Inst., Amsterdam, The Netherlands, Jul. 2004, [Online]. Available: https://ideas.repec.org/p/tin/wpaper/20040079.html

[8] M. Balbo and G. Marconi, "International migration, diversity and urban governance in cities of the South," *Habitat Int.*, vol. 30, no. 3, pp. 706–715, 2006.

[9] U. E. Ekpenyong, J. Zhang, and X. Xia, "How information propagation in social networks can improve energy savings based on time of use tariff," *Sustain. Cities Soc.*, vol. 19, pp. 26–33, 2015.

[10] J. Zeng, "The optimization of industrial structure of urban agglomeration from the perspective of spatial interaction: Case study of Wuhan urban agglomeration," *Econ. Geogr.*, vol. 33, no. 7, pp. 102–108, 2013.

[11] S. Zhang, D. Zhu, X. Yao, X. Cheng, H. He, and Y. Liu, "The scale effect on spatial interaction patterns: An empirical study using taxi O-D data of Beijing and Shanghai," *IEEE Access*, vol. 6, pp. 51994–52003, 2018.

[12] G. Bruno and A. Genovese, "A spatial interaction model for the representation of the mobility of university students on the Italian Territory," *Netw. Spatial Econ.*, vol. 12, pp. 41–57, 2012.

[13] A. D. Singleton, A. G. Wilson, and O. O'Brien, "Geodemographics and spatial interaction: An integrated model for higher education," *J. GeoGraphical Syst.*, vol. 14, no. 2, pp. 223–241, 2012.

[14] M. De Beule, D. Van den Poel, and N. Van de Weghe, "An extended Huff-model for robustly benchmarking and predicting retail network performance," *Appl. Geography*, vol. 46, pp. 80–89, 2014.

[15] L. Avery, "Rural-Urban connectivity in achieving sustainable regional development," in *Proc. Intergovern. 10th Region. Environ. Sustain. Transp. (EST) Forum*, Asia, 2017.

[16] H. Matsumoto, "International urban systems and air passenger and cargo flows: Some calculations," *J. Air Transp. Manage.*, vol. 10, no. 4, pp. 239–247, 2004.

[17] Y. Xiao, F. Wang, Y. Liu, and J. Wang, "Reconstructing gravitational attractions of major cities in China from air passenger flow data, 2001–2008: A particle swarm optimization approach," *Prof. Geographer*, vol. 65, no. 2, pp. 265–282, 2013.

[18] J. Wang, H. Mo, and F. Wang, "Evolution of air transport network of China 1930–2012," *J. Transport Geography*, vol. 40, pp. 145–158, 2014.

[19] L. Shiwei, F. Zhixiang, S. Shih-Lung, and Z. Xirui, "Impacts of high-speed rails on the accessibility inequality of railway network in China," in *Proc. 22nd Int. Conf. Geoinformat.*, 2014, pp. 1–5.

[20] A. De Montis, M. Barthélemy, A. Chessa, and A. Vespignani, "The structure of interurban traffic: A weighted network analysis," *Environ. Plan. B, Plan. Des.*, vol. 34, no. 5, pp. 905–924, 2007.

[21] P. Kaluza, A. Kölzsch, M. T. Gastner, and B. Blasius, "The complex network of global cargo ship movements," *J. Roy. Soc. Interface*, vol. 7, no. 48, pp. 1093–1103, 2010.

[22] A. Vasanen, "Functional polycentricity: Examining metropolitan spatial structure through the connectivity of urban sub-centres," *Urban Stud.*, vol. 49, no. 16, pp. 3627–3644, 2012.

[23] A. Mazza and A. Punzo, "Spatial attraction in migrants' settlement patterns in the city of Catania," *Demographic Res.*, vol. 35, no. 5, pp. 117–138, 2016.

[24] M. R. Sanderson, B. Derudder, M. Timberlake, and F. Witlox, "Are world cities also world immigrant cities? An international, cross-city analysis of global centrality and immigration," *Int. J. Comp. Sociol.*, vol. 56, no. 3–4, pp. 173–197, 2015.

[25] Y. Liu, Z. Sui, C. Kang, and Y. Gao, "Uncovering patterns of Inter-Urban trip and spatial interaction from social media check-in data," *PLoS ONE*, vol. 9, no. 1, 2014, Art. no. e86026.

[26] R. Huggins and D. Prokop, "Network structure and regional innovation: A study of university–industry ties," *Urban Stud.*, vol. 54, no. 4, pp. 931–952, 2017.

[27] F. Zhen, B. Wang, and Y. Chen, "China's city network characteristics based on social network space: An empirical analysis of Sina micro-blog," *Acta Geographica Sinica*, vol. 67, pp. 1031–1043, 2012.

[28] L. Lu and R. Huang, "Urban hierarchy of innovation capability and intercity linkages of knowledge in post-reform China," *Chin. Geographical Sci.*, vol. 22, pp. 606–616, 2012.

[29] M. Burger and E. Meijers, "Form follows function? Linking morphological and functional polycentricity," *Urban Stud.*, vol. 49, no. 5, pp. 1127–1149, 2012.

[30] X. Liu *et al.*, "High-resolution multi-temporal mapping of global urban land using landsat images based on the Google Earth Engine platform," *Remote Sens. Environ.*, vol. 209, pp. 227–239, 2018.

[31] D. C. C. John and R. Jensen "Remote sensing of urban/Suburban infrastructure and socio-economic attributes," in *The Map Reader: Theories of Mapping Practice and Cartographic Representation*, M. Dodge, R. Kitchin, and C. Perkins, Eds., New York, NY, USA: Wiley, 2011, pp. 153–163.

[32] Z. Xia, X. Li, Y. Zhou, and D. Li, "Analyzing Urban spatial connectivity using night light observations: A case study of three representative urban Agglomerations in China," *IEEE J. Sel. Topics Appl. Earth Observ. Remote Sens.*, vol. 13, pp. 1097–1108, 2020.

[33] Z. Chen *et al.*, "Mapping global Urban areas from 2000 to 2012 using time-series nighttime light data and MODIS products," *IEEE J. Sel. Topics Appl. Earth Observ. Remote Sens.*, vol. 12, no. 4, pp. 1143–1153, Apr. 2019.

[34] K. Shi *et al.*, "Urban expansion and agricultural land loss in China: A multiscale perspective," *Sustainability*, vol. 8, no. 8, pp. 790, 2016.

[35] B. Yu *et al.*, "Urban built-up area extraction from log-transformed NPP-VIIRS nighttime light composite data," *IEEE Geosci. Remote Sens. Lett.*, vol. 15, no. 8, pp. 1279–1283, Aug. 2018.

[36] Y. Liu, T. Delahunty, N. Zhao, and G. Cao, "These lit areas are undeveloped: Delimiting China's urban extents from thresholded nighttime light imagery," *Int. J. Appl. Earth Observ. Geoinf.*, vol. 50, pp. 39–50, 2016.

[37] Z. Chen *et al.*, "A new approach for detecting urban centers and their spatial structure with nighttime light remote sensing," *IEEE Trans. Geosci. Remote Sens.*, vol. 55, no. 11, pp. 6305–6319, Nov. 2017.

[38] Y. Li and X. Liu, "How did urban polycentricity and dispersion affect economic productivity? A case study of 306 Chinese cities," *Landscape Urban Plan.*, vol. 173, pp. 51–59, 2018.

[39] C. Yang *et al.*, "A spatial-socioeconomic urban development status curve from NPP-VIIRS nighttime light data," *Remote Sens.*, vol. 11, no. 20, p. 2398, 2019.

[40] Z. Chen *et al.*, "Delineating seasonal relationships between Suomi NPP-VIIRS nighttime light and human activity across Shanghai, China," *IEEE J. Sel. Topics Appl. Earth Observ. Remote Sens.*, vol. 12, no. 11, pp. 4275–4283, Nov. 2019.

[41] K. Shi, Z. Chang, Z. Chen, J. Wu, and B. Yu, "Identifying and evaluating poverty using multisource remote sensing and point of interest (POI) data: A case study of Chongqing, China," *J. Clean Prod.*, vol. 255, 2020, Art. no. 120245.

[42] K. Shi *et al.*, "Modeling spatiotemporal CO_2 (carbon dioxide) emission dynamics in China from DMSP-OLS nighttime stable light data using panel data analysis," *Appl. Energy*, vol. 168, pp. 523–533, 2016.

[43] Y. Liu, G. Cao, N. Zhao, K. Mulligan, and X. Ye, "Improve ground-level PM2.5 concentration mapping using a random forests-based geostatistical approach," *Environ. Pollut.*, vol. 235, pp. 272–282, 2018.

[44] X. Zhao *et al.*, "NPP-VIIRS DNB daily data in natural disaster assessment: Evidence from selected case studies," *Remote Sens.*, vol. 10, no. 10, p. 1526, 2018.

[45] N. Zhao *et al.*, "Time series analysis of VIIRS-DNB nighttime lights imagery for change detection in urban areas: A case study of devastation in Puerto Rico from hurricanes Irma and Maria," *Appl. Geography*, vol. 120, 2020, Art. no. 102222.

[46] Y. Huang, K. Shi, H. Zong, T. Zhou, and J. Shen, "Exploring spatial and temporal connection patterns among the districts in Chongqing based on highway passenger flow," *Remote Sens.*, vol. 12, no. 1, p. 27, 2019.

[47] E. G. Ravenstein, "The laws of migration," *J. Statist. Soc.*, vol. 48, no. 2, pp. 167–227, 1885.

[48] W. J. Reilly, *Methods for the Study of Retail Relationships* (Bureau of Business Research Research Monograph, no. 4). University of Texas Bulletin: The University of Texas Austin, 1929.

[49] P. D. Converse, "New laws of retail gravitation," *J. Marketing*, vol. 14, no. 3, pp. 379–384, 1949.

[50] A. G. Wilson, *Entropy in Urban and Regional Modelling*, vol. 42, London, U.K.: Pion Press, 1970.

[51] A. G. Wilson, "A family of spatial interaction models, and associated developments," *Environ. Plan. A, Econ. Space*, vol. 3, no. 1, pp. 1–32, 1971.

[52] W. Alonso, *National Interregional Demographic Accounts: A Prototype*, Berkeley, CA, USA: Inst. Urban Regional Develop., (in English), 1973.

[53] D. L. Huff, "Defining and estimating a trading area," *J. Marketing*, vol. 28, no. 3, pp. 34–38, 1964.

[54] I. S. Lowry, *A Model of Metropolis*. Santa Monica, CA, USA: RAND Corp., 1964.

[55] M. M. Fischer and S. Gopal, "Artificial neural networks: A new approach to modelling interregional telecommunication flows," *J. Regional Sci.*, vol. 34, no. 4, pp. 503–527, 1994.

[56] B. R. Tripathy *et al.*, "Estimation of urban population dynamics using DMSP-OLS night-time lights time series sensors data," *IEEE Sensors J.*, vol. 17, no. 4, pp. 1013–1020, Feb. 2017.

[57] B. Yu *et al.*, "Integration of nighttime light remote sensing images and taxi GPS tracking data for population surface enhancement," *Int. J. Geographical Inf. Sci.*, vol. 33, no. 4, pp. 687–706, 2018.

[58] J. He, "Implementation of the Shanghai master plan (2001-2020)," in *AESOP 26th Ann. Congress*, Ankara, 2012.

[59] K. Shi *et al.*, "Evaluating the ability of NPP-VIIRS nighttime light data to estimate the gross domestic product and the electric power consumption of China at multiple scales: A comparison with DMSP-OLS data," *Remote Sens.*, vol. 6, no. 2, pp. 1705–1724, Feb. 2014.

[60] D. Xia *et al.*, "Discovering spatiotemporal characteristics of passenger travel with mobile trajectory big data," *Physica A, Statist. Mech. Appl.*, vol. 578, 2021, Art. no. 126056.

[61] Y. Zhang *et al.*, "A global north-south division line for portraying urban development," *iScience*, vol. 24, no. 7, 2021, Art. no. 102729.

[62] S. Zhang, J. Tang, H. Wang, Y. Wang, and S. An, "Revealing intra-urban travel patterns and service ranges from taxi trajectories," *J. Transport Geography*, vol. 61, pp. 72–86, 2017.

[63] G. Giuliano and K. A. Small, "Subcenters in the Los Angeles region," *Regional Sci. Urban Econ.*, vol. 21, no. 2, pp. 163–182, 1991.

[64] M. Wang, B. Derudder, and X. Liu, "Polycentric urban development and economic productivity in China: A multiscalar analysis," *Environ. Plan. A, Econ. Space*, vol. 51, no. 8, pp. 1622–1643, 2019.

Yue Tu received the B.S. degree in geographical science from Huanggang Normal University, Huanggang, China, in 2018. She is currently working toward the M.S. degree in geography with the Key Laboratory of Spatial Data Mining and Information Sharing of Ministry of Education, the Academy of Digital China, Fuzhou University, Fuzhou, China.

Her research interests include urban remote sensing, nighttime light remote sensing and data mining.

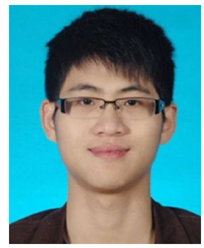

Zuoqi Chen (Member, IEEE) received the B.S. degree in geographic information system from Fujian Normal University, Fuzhou, China, in 2011, and the Ph.D. degree in cartography and geographic information system from East China Normal University, Shanghai, China, in 2017.

He is currently an Assistant Research Fellow with the Key Laboratory of Spatial Data Mining and Information Sharing of Ministry of Education, and the Academy of Digital China, Fuzhou University, Fuzhou, China. His research interests include urban remote sensing, nighttime light remote sensing, and development of geographic information system.

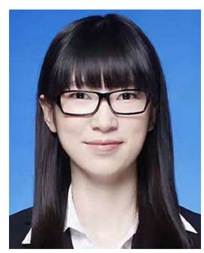

Congxiao Wang received the B.S. and M.S. degrees in cartography and geographic information system from Shanghai Normal University, Shanghai, China, in 2014 and 2017, respectively. She is currently working toward the Ph.D. degree in cartography and geographic information system with East China Normal University, Shanghai, China.

Her research interests include nighttime light remote sensing and its application in urban research.

Bailang Yu (Senior Member, IEEE) received the B.S. and Ph.D. degrees in cartography and geographic information systems from East China Normal University, Shanghai, China, in 2002 and 2009, respectively.

He is currently a Professor with the Key Laboratories of Geographic Information Science, Ministry of Education, the School of Geographic Sciences, East China Normal University. His research interests include urban remote sensing, nighttime light remote sensing, Lidar, and object-based methods.

Bingjie Liu received the B.S. degree in surveying and mapping engineering from Henan Polytechnic University, Jiaozuo, China, in 2018, and the M.S. degree in surveying and mapping engineering from the Key Laboratory of Spatial Data Mining and Information Sharing of Ministry of Education, and the Academy of Digital China, Fuzhou University, Fuzhou, China, in 2021.

Her research interests include urban remote sensing, nighttime light remote sensing and Data Mining.